Journal of Energy Storage 72 (2023) 108412

Contents lists available at ScienceDirect

Journal of Energy Storage

journal homepage: www.elsevier.com/locate/est

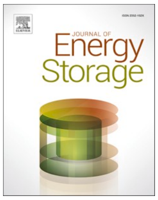

Research papers

Experimental evaluation of the thermal degradation of solar salt under different gas covers

Cristina Prieto [a,*], Anton Lopez-Roman [a], Luisa F. Cabeza [b]

[a] *Department of Energy Engineering, Universidad de Sevilla, 41092 Sevilla, Spain*
[b] *GREiA Research Group, Universitat de Lleida, Pere de Cabrera s/n, 25001 Lleida, Spain*

ARTICLE INFO

Keywords:
Solar salt
Thermal decomposition
Cover gas
Concentrating solar power (CSP)
Thermal energy storage (TES)

ABSTRACT

Commercial concentrating solar power (CSP) plants use solar salt (60–40 wt% $NaNO_3$-KNO_3) as thermal energy storage media due to its proven performance. Nevertheless, at high temperatures its decomposition can become a problem, hindering the possibility to rise operating temperatures. Therefore, this paper studies the decomposition of solar salt using different cover gases, dry air and oxygen. Results show that the use of oxygen as cover gas, instead the commercially used dry air, slows down the thermal decomposition of solar salt, reducing the amount of NOx and nitrites formation.

1. Introduction

The use of the nitrate binary salt named solar salt (60–40 wt% $NaNO_3$-KNO_3) has demonstrated its validity as thermal energy storage fluid in the gigawatt-hour scale (234 GWh of TES capacity by the end of 2019 and to be increased threefold by 2030 [1]). Up to date, its working range lies between 280 and 565 °C ([2,3]). The lower temperature of this range is related to freezing issues of the salt, while the upper range was defined by general consensus in the concentrating solar power (CSP) industry after research at different scales. This temperature, around 565 °C, is supposed to be the maximum temperature where, in open atmospheres, the decomposition reactions can affect the integrity of the salt. The maximum temperature is directly related to the volumetric storage capacity and to the efficiency of the coupled steam power cycle, and thus maximizing it has clear benefits on the system.

The mechanism of the thermal decomposition of solar salt is described in the literature [4–8] and can be summarized with the following reactions:

(a) Decomposition at liquid phase

$$NO_3^- \leftrightarrow NO_2^- + {}^1\!/\!{}_2 O_{2(g)} \tag{1}$$

$$\left(NO_3^-\right)_2 \leftrightarrow O^- + 2NO_{2(g)} + {}^1\!/\!{}_2 O_{2(g)} \tag{2}$$

$$\left(NO_3^-\right)_2 \leftrightarrow O^{2-} + N_2O_{(g)} + 2O_{2(g)} \tag{3}$$

$$2NO_2^- \leftrightarrow O^{2-} + NO_{(g)} + NO_{2(g)} \tag{4}$$

$$2NO_2^- \leftrightarrow O^{2-} + {}^3\!/\!{}_2 O_{2(g)} + N_{2(g)} \tag{5}$$

$$NO_2^- + NO_{(g)} \leftrightarrow NO_3^{2-} + N_{2(g)} \tag{6}$$

(b) Dissociation reaction at liquid phase

$$NO_3^- \leftrightarrow NO_2^+ + O^{2-} \tag{7}$$

$$NO_2^- \leftrightarrow NO^+ + O^{2-} \tag{8}$$

(c) Oxidation at gaseous phase

$$NO_{(g)} + {}^1\!/\!{}_2 O_{2(g)} \leftrightarrow NO_{2(g)} \tag{9}$$

Typically, the CSP industry uses dry air as cover gas in direct TES tanks. While this solution has been commercially proven, this paper studies the differences in decomposition of solar salt using different cover gases aiming to increase the operating temperature of the available commercial solutions with minimum modifications.

Since the products of the decomposition of solar salt are O_2 and NO_x, the first approach to inhibit such decomposition is to use either O_2 or NO_x as cover gas. While the use of NO_x as cover gas may look like a suitable option, the restrictive legislation on NO_x emissions coupled with the need to periodically release the cover gas during operation

---

* Corresponding author at: Department of Energy Engineering, Universidad de Sevilla, 41092 Sevilla, Spain.
E-mail address: cprieto@us.es (C. Prieto).

https://doi.org/10.1016/j.est.2023.108412
Received 9 January 2023; Received in revised form 9 June 2023; Accepted 14 July 2023

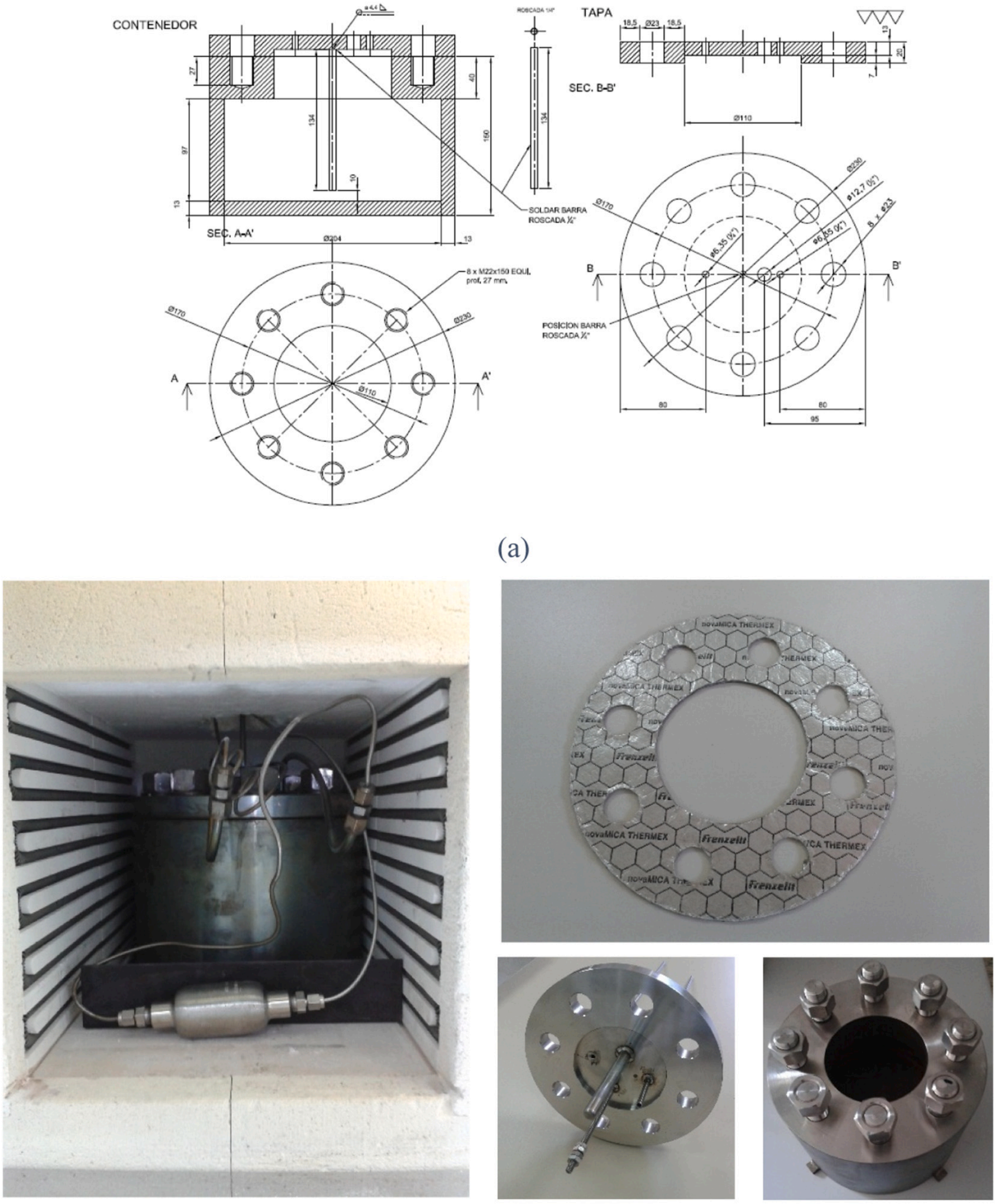

Fig. 1. Tank designed and used for the experimentation. (a) Design; (b) photos.

Fig. 2. Experimental test rig.

makes it not commercially viable. Therefore, this paper studies the use of O_2 as cover gas and evaluates it in comparison with the commercial cover gas solution, dry air.

2. Materials and methodology

2.1. Materials

Solar salt 60 wt% sodium nitrate and 40 wt% potassium nitrate, supplied by SQM® (Sociedad Quimica y Minera) in powder form with refined quality. In order to prepare the sample for the essay, a significant quantity of this powder (around 50 g) was melted and homogenized at 300 °C for 2 h.

2.2. Description of the experimental rig

A new test rig is designed and built for the experiment. The core component is a tank able to store 4 kg of solar salt (Fig. 1) and to heat it up to 650 °C. The tank has a total volume of 3.62 l and is made of Inconel 600, the other parts of the test rig are made of stainless steel 316L and 304L.

Table 1
Instruments description.

Description	Supplier	Range
Thermocouples (type K Inconel 600)	Jumo	−200–1300 °C
RTD (dTRANS)	Jumo	−40–100 °C
Pressure transmitter (Midas)	Jumo	0–4 bar 0–25 bar
Pressure drop transmitter (dTRANS p02)	Jumo	0–60 mbar
Rupture disk	Fike	3 bar at 400 °C
NO_x analyser (Testo 340)	Testo 340	

Table 2
Construction materials in piping and tank.

Exchanger/element	PIPE code Material 316L	ODxwall thickness (inch)
Air, O_2 inlet	SS-T2-S-028-6ME	$^{1}/_{8}$" ODx0.028
Gas outlet	SS-T2-S-028-6ME	$^{1}/_{8}$" ODx0.028
Gas outlet	SS-T4-S-035-6ME	¼" ODx0.035

Tank	Element code	Material
Tank (650 °C)	Inconel 600	Inconel 600
Salt reservoir/trap	304L-HDF4-50	SS304L

The test rig (Figs. 2 and 3) can provide dry air or oxygen as cover gas at 30 mL/min, controlled by an Omega rotameter. The tank holding the salt to be tested is kept inside a Carbolite oven, model CSF 11/23 PI, able to keep the temperature at 1100 ± 5 °C with 7000 W of maximum power. The gas exiting the tank (mix of the cover gas and produced gases) is cooled down in a long enough pipe before being analysed (Tables 1 and 2).

2.3. Methodology

The salt was heated up to 650 °C with two different cover gases, oxygen and dry air. The gas flow is approximately 30 mL/min for 750 h. The process has three stages, first (i) the tank is kept at 165–200 °C for 12 h to ensure that the salt is dehydrated, and then, (ii) the tank is heated up to 450 °C. In these two states the cover gas is always dry air. In the third stage (iii) the tank is heated up to 650 °C with either dry air or oxygen. The outlet gases produced at 450 °C and at 600 °C are analysed. Finally, the salt remaining after the test is finished is analysed.

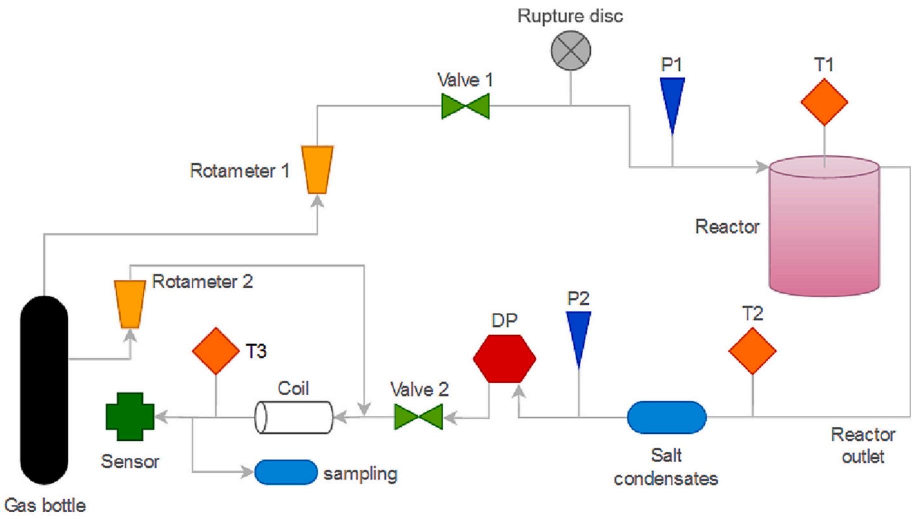

Fig. 3. Experimental setup diagram.

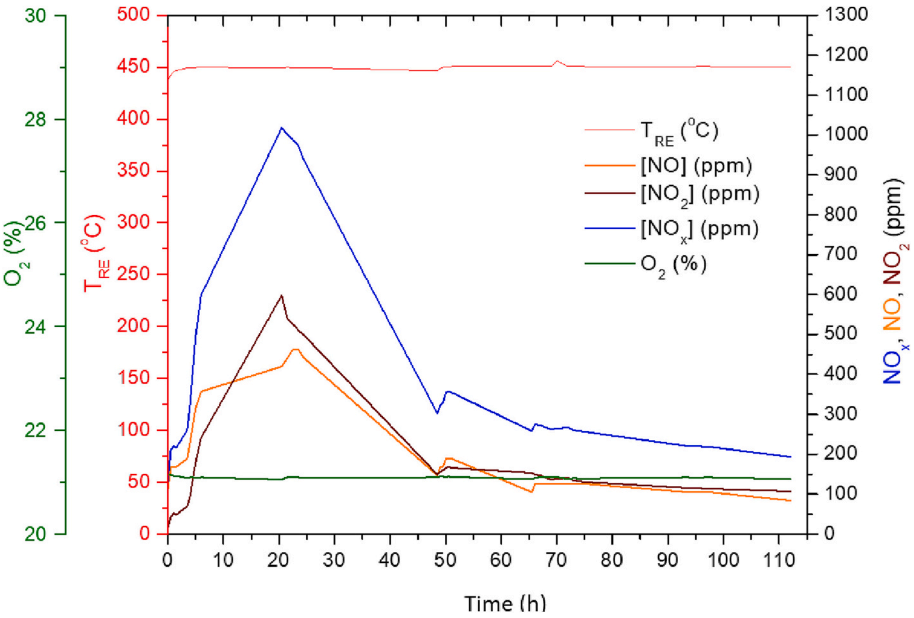

Fig. 4. Concentration of outlet gases during the heating process - Concentration of NOx referred to the 30 mL/min flow. Concentration of oxygen referred to the diluted concentration (30 mL/min O_2 + 600 mL/min air).

2.4. Analytical methods

The NOx content of the outlet gases is analysed with a TESTO 340 analyser. The minimum flow required by the manufacturer is 600 mL/min. Since the outlet flow of the reactor is 30 mL/min, the flow is diluted with 600 mL/min of air prior injecting it into the analyser. The salt is analysed using a thermogravimetric analyser (TGA) Seiko, model Exstar 6000 and a differential scanning calorimeter (DSC) TA Instruments, model Q100. For both equipment, the heating rate is 10 K/min. The TGA process uses a heating range 50–1000 °C, with nitrogen as cover gas at 100 mL/min. In the DSC, a sample of 5–20 mg is placed inside a hermetic aluminium crucible with a heating range of 150–270 °C, and nitrogen as cover gas at 50 mL/min.

The nitrites content produced in the thermal degradation is measured with ionic chromatography, model Dionex Ion Chromatograph with a UV Visible absorbance detector.

3. Results

3.1. Oxygen as cover gas

The salt is dehydrated in a separated oven at 200 °C during 24 h and then a second dehydration process is performed at 165–200 °C for 12 h in the reactor. Next, the temperature is raised to 450 °C using 30 mL/min of synthetic air during the whole process. The gas generated during this process while the magnesium nitrates are being decomposed is analysed [9]. There is a maximum of NOx emissions after 20 h at 450 °C with a NO_x concentration of 1000 ppm, which is reduced after 110 h down to 200 ppm maintaining the same temperature (Fig. 4). At the beginning of this period, the concentration of NO is slightly higher than that of NO_2, but later both gases have similar concentration (Fig. 5).

After 110 h at 450 °C, the cover gas is changed to oxygen and, as it can be seen in Fig. 5, the concentration of NO_x decreased slightly. After 1 h of stabilization, the temperature is increased to 650 °C (this process took about 4 h). Fig. 5a shows the concentration of gases produced during the heating process from 450 °C to 650 °C, showing a peak of about 27,000 ppm at 585 °C in the process. Fig. 5b is a zoom-in of Fig. 5a of the last 650 h of the experiment at 650 °C, showing a detail of the concentration of the produced gases. As it can be seen in this figure, after 300 h of treatment the NOx concentration reaches an asymptotic value of 500 ppm, with the concentration of NO higher than that of NO_2. During this whole process, more gases are produced inside the tank than in the previous step (heating up to 450 °C with air), increasing the overall pressure in the tank. Despite this, the inlet flow is kept constant at 30 mL/min of O_2 for the whole experiment.

After 750 h at 650 °C, the tank is cooled down. During this process, no outlet gases are produced even though 30 mL/min of O_2 are used as cover gas for the whole period.

Fig. 6a shows the TGA of the salt before treatment (SF) and after treatment (SD) for two samples (01–02). Both, the salt before and after treatment behaved very similar, there is a weight decrease at low temperatures (below 150 °C), probably due to water evaporation, and a thermal decomposition at 624.0 ± 2.5 °C, when a weight loss of about 5 wt% was observed. Fig. 6b shows the results obtained with DSC for both cases. The case treated at 650 °C for 750 h with O_2 as cover gas has a lower melting temperature (214 °C) than the salt without treatment (vs. 227 ± 0.5 °C).

Fig. 6 and Table 3 show that the melting temperature of the molten salt obtained through DSC in the heating ramp is slightly reduced with respect to the raw sample on 13 ± 0.5 °C. As it is explained later in Fig. 7, this technique detected at least two different melting enthalpies, probably due to the presence of different compounds. In both cases, the temperatures shown in Table 3 are related to the minimum of the first melting spikes.

3.2. Dry air as cover gas

The same procedure used for the oxygen case is replicated for the air as cover gas: the salt is dehydrated in a separated oven at 200 °C during 24 h, then introduced into the test plant and heated at 165–200 °C for 12 h. After this second dehydration phase, the salt is heated to 450 °C. All the process is done with 30 mL/min of dry air as cover gas. The outlet gas obtained during this last period is analysed (Fig. 7a), measuring a maximum of NO_x production after 7 h at 450 °C (with a concentration of 1200 ppm of NOx). During this phase, the NO concentration is higher than the concentration of NO_2 at the beginning, but it becomes similar after around 7 h, both decreasing constantly until the NOx concentration reaches 180 ppm at 165 h with a slightly higher contribution from NO_2

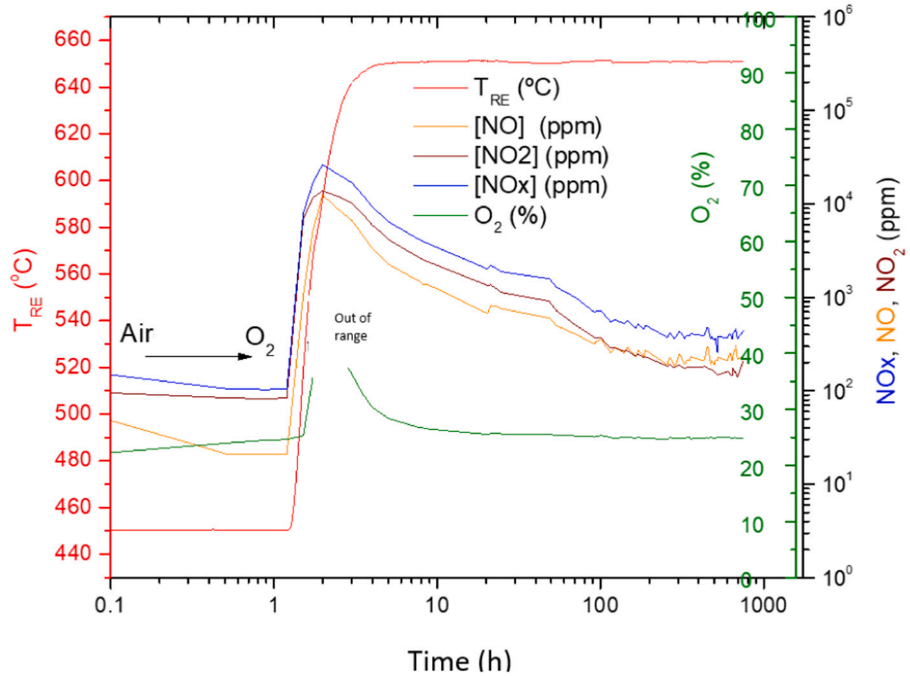

(a)

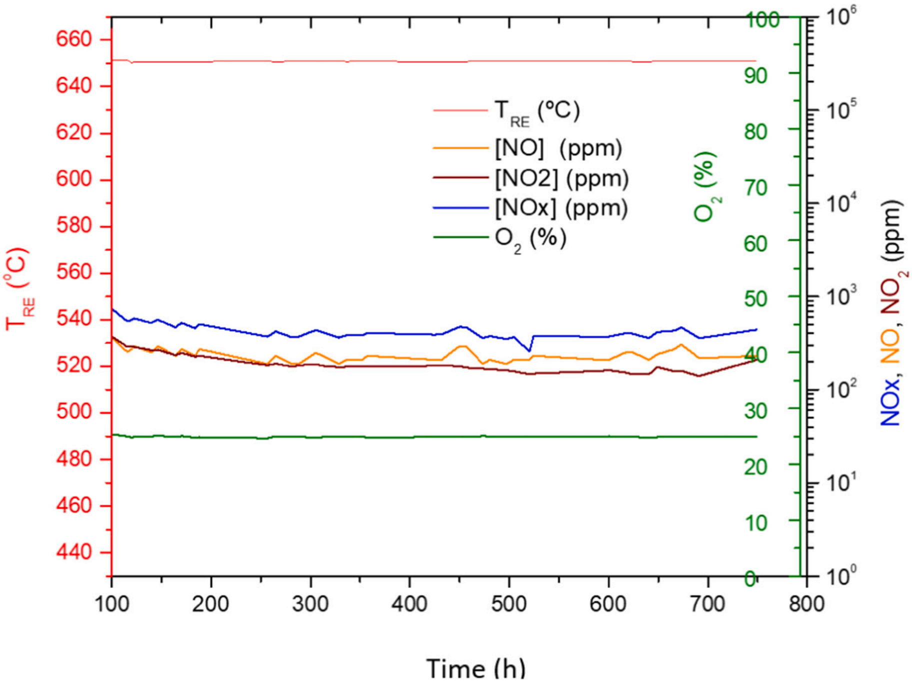

(b)

Fig. 5. Concentration of outlet gases using oxygen as cover gas (a) during the heating process between 450 °C and 650 °C; and (b) during the heating process at 650 °C for 750 h - Concentration of NOx referred to the 30 mL/min flow. Concentration of oxygen referred to the diluted concentration (30 mL/min O_2 + 600 mL/min air).

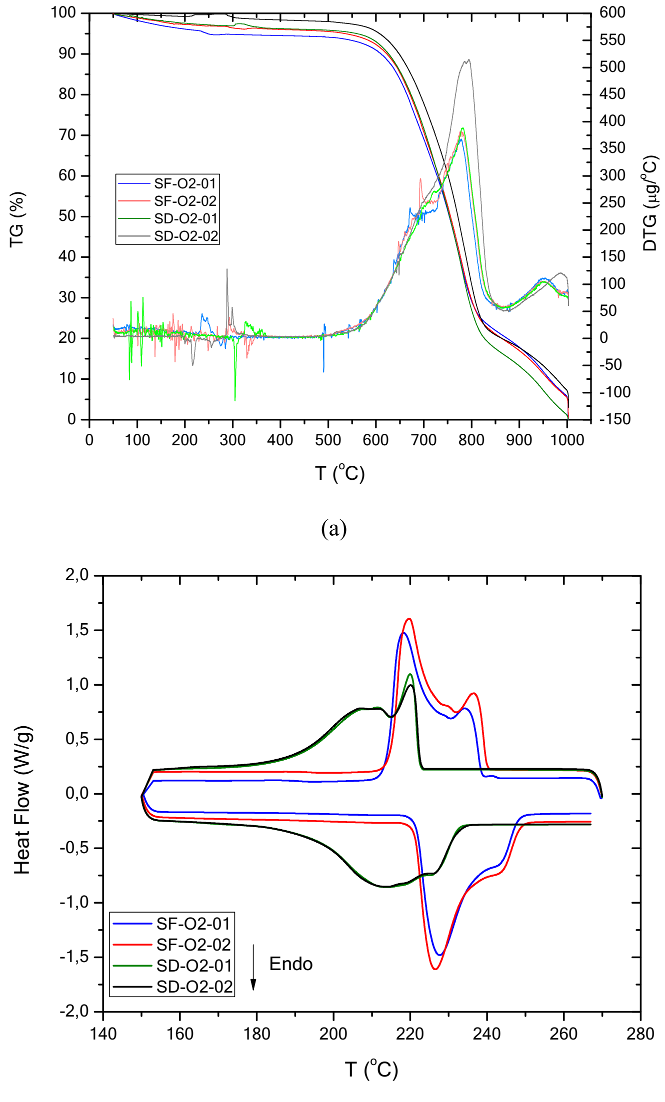

(a)

(b)

Fig. 6. Analysis of the solar salt before and after treatment with oxygen as cover gas. (a) TGA and (b) DSC. SF salt before treatment; SD salt after treatment; 01 and 02 two samples for each case.

Table 3
Results for raw and degraded salts at 650 °C for 750 h in a O_2 atmosphere.

Salt	$T_{melting}$ (°C) by DSC	$T_{melting}$ (°C) by TGA	Decomposition (°C)
Raw sample	227.0 ± 0.5	227.5 ± 0.5	624.0
Degraded	214.0	209.5 ± 1.5	624.0 ± 4.2

than from NO.

After the isothermal period at 450 °C, the salt is, as in the previous case, heated to 650 °C with a heating time of 4 h. As it happened in the previous experiment, during this heating phase the production of gases is significant, with a peak of NO_x of 34,800 ppm at 590 °C, and a partial concentration of O_2 in the diluted current of 66.72 vol% (Fig. 7b). During the heating transient from 450 °C to 650 °C, the concentration of NO_2 is almost always higher than the concentration of NO, changing this behaviour after the temperature is stabilized. After 750 h at 650 °C, the concentration of NO_2 reached very low values at around 15 ppm while the concentration of NO is kept quite stable at around 200 ppm (Fig. 7c).

Fig. 8a shows the TGA analysis of the salt before and after treatment during 750 h at 650 °C for two samples per case (01–02). Both cases behave very similar, with a weight loss at the beginning, probably due to water evaporation. The measured decomposition temperatures are 636.5 ± 4.5 °C for the salt before treatment and 634.7 ± 1.8 °C for the salt after treatment. Fig. 8b shows the DSC analysis of the salt before and after treatment. Here there is a clear difference between both cases. The salt before treatment had a melting temperature of 226.3 ± 0.3 °C and the salt after treatment had a melting temperature of 198.4 ± 0.3 °C, showing an important degradation in the salt due to the treatment.

The results of the DSC (Fig. 8) show the expected thermogram for a 40/60 ($KNO_3/NaNO_3$) molten salt, with the presence of two melting temperature due to different crystalline phases. For the melting temperatures of the salt obtained by DSC (Table 4), the test with air shows an important reduction on the melting temperature of the degraded salt with respect to its raw counterpart of 27.9 ± 0.3 °C.

4. Discussion

The literature [10] shows that the mixture of $KNO_3/NaNO_3$ (solar salt) has different melting behaviour depending on its concentration (Fig. 9). The same behaviour was measured, finding that, depending on the amount of solar salt used, the melting profile varies (Fig. 10). In this experiment, the mixture of 2 g gave a proportion of $KNO_3/NaNO_3$ close to the eutectic point (50/50), while the samples with higher weight gave concentrations closer to the commercial solar salt used (40/60).

Fig. 11 shows the concentration of the gases generated during the heating ramp from 450 °C to 650 °C and the isothermal period at 650 °C for both tests, with oxygen as cover gas (E1) and with dry air as cover gas (E2). The concentration of NOx is related to 30 mL/min and for the O_2 is related to the diluted gas (600 + 30 mL/min). The fast temperature increase can be explained by the decomposition of the solar salt with the production of oxygen and NOx [8]. The main decomposition mechanism in this process is the described by Eqs. (1), (4), and (5) [5,6].

In the heating period at 650 °C, the evolution in NO_x concentration in both cover gases is very similar (Fig. 12). Nevertheless, the concentration of NO_x is 22.4 % higher when dry air is used as cover gas (34,800 ppm) than when oxygen is used (27,000 ppm). For NO_2 this concentration is 18.2 % higher, and for NO is 32.8 % higher. These results are in line with the literature [6,7], that states that the oxygen partial pressure limits the transition from nitrate to nitrite due to the decomposition of the salt and later decomposition of nitrites into NO and NO_2 (Eqs. (4) and (5)).

After enough time has passed and the stationary state is reached (at 650 °C and after 750 h), the degradation process seems to stabilise, showing an asymptotic trend of NOx production of around 500 ppm (for an inlet flow of 30 mL/min) for the oxygen atmosphere, while for the air atmosphere this production is lower, at 200 ppm. There are several authors that try to describe the complexity of the different possible decomposition processes, even more when, as in this case, the reactor atmosphere is being extracted slowly (at 30 mL/min) and heating/cooling processes in the reactor have a high thermal inertia. To understand the reactions happening (and the lower NOx emissions on the air test), it is required to fully understand the composition of the degraded salt (nitrates, nitrites, oxides, etc.) both in the oxygen case and in the air case described in this paper, but also in other experimentations performed under more controlled conditions.

In this line, the presence of nitrites in the degraded salt after these experiments was analysed by ionic chromatography, and the results obtained are shown in Table 5. As seen, the presence of nitrites in the degraded salt (E1) is almost three times (2.8 times) the present in the oxygen test (E2).

These results are again in line with the fact that the higher oxygen partial pressure limits the decomposition of nitrates to nitrites [5]:

$$K = \frac{[NO_3^-]}{[NO_2^-]} \cdot P_{O_2}^{-1/2} \tag{10}$$

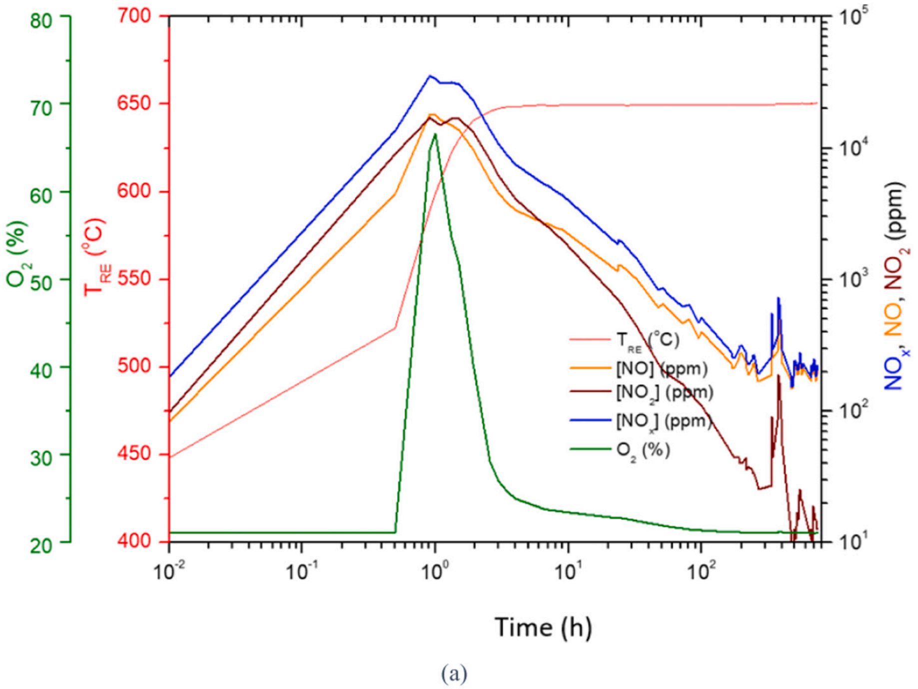

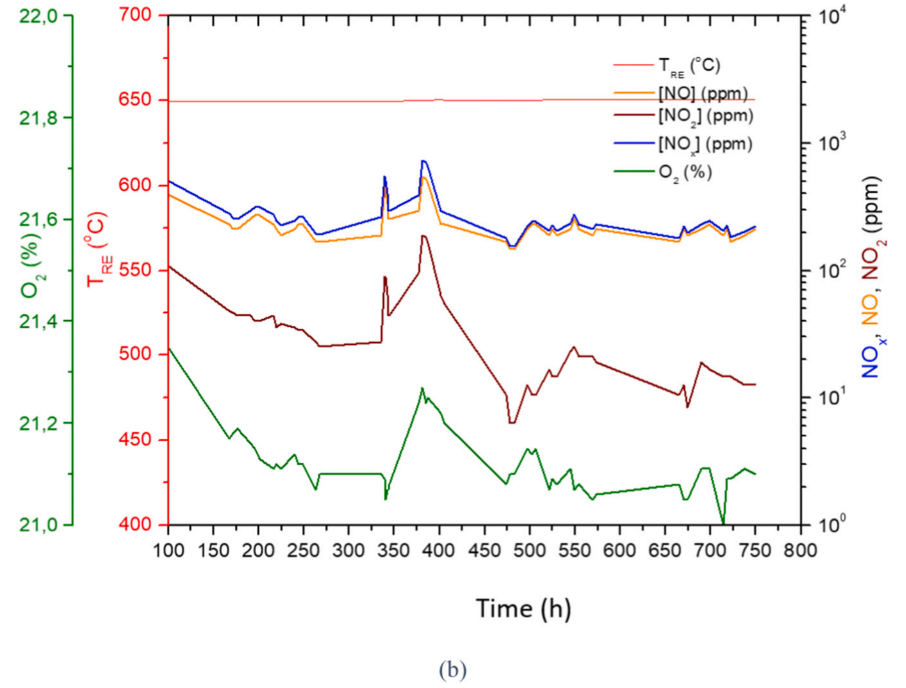

Fig. 7. Concentration of outlet gases using dry air as cover gas (a) during the heating process between 450 °C and 650 °C; and (b) during the heating process at 650 °C for 750 h - Concentration of NOx referred to the 30 mL/min flow. Concentration of oxygen referred to the diluted concentration (30 mL/min O_2 + 600 mL/min air).

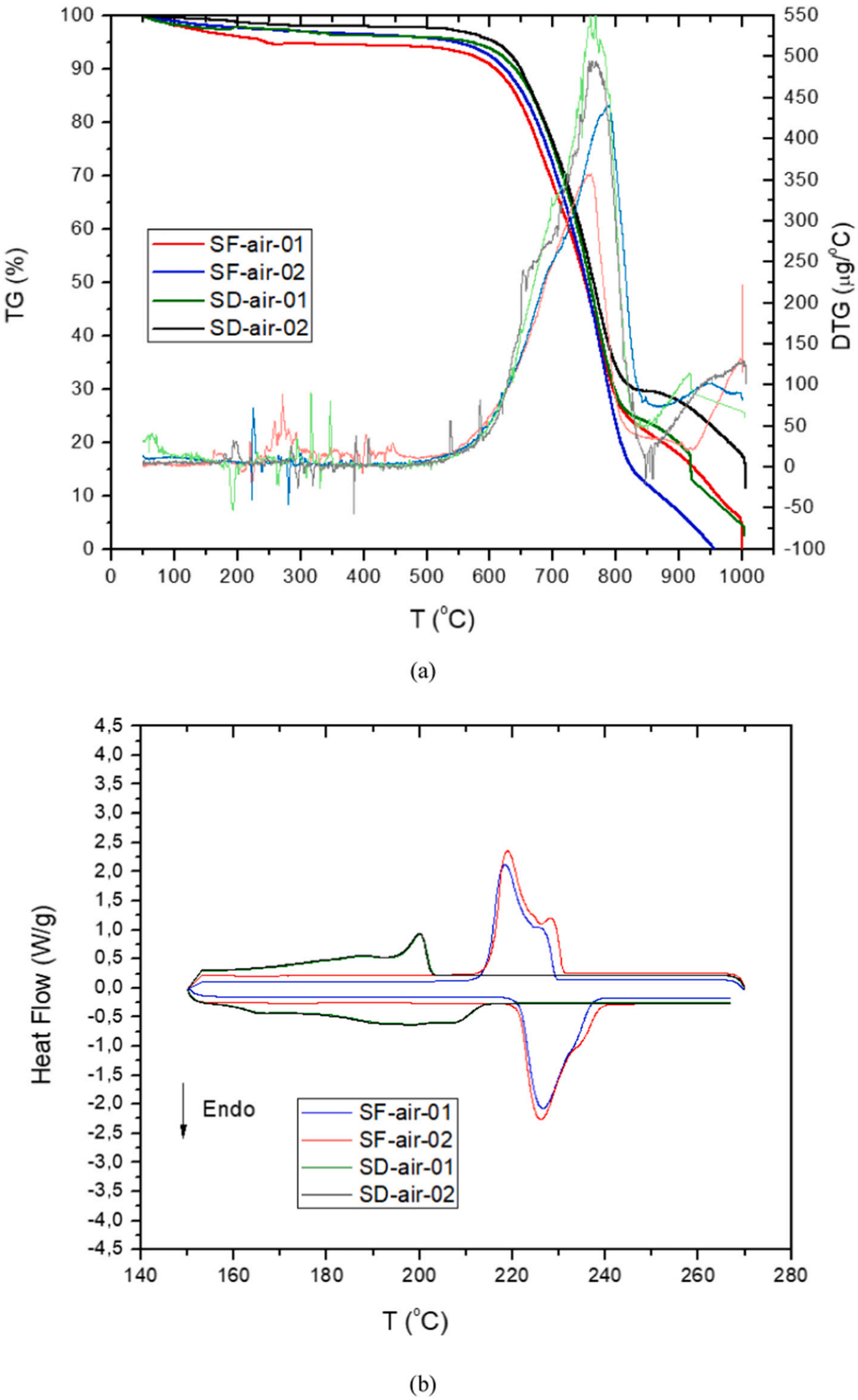

Fig. 8. Analysis of the solar salt before and after treatment with dry air as cover gas. (a) TGA and (b) DSC. SF salt before treatment; SD salt after treatment; 01 and 02 two samples for each case.

Table 4
Results for raw and degraded salts at 650 °C for 750 h in air atmosphere.

Salt	$T_{melting}$ (°C) by DSC	$T_{melting}$ (°C) by TGA	Decomposition (°C)
Raw sample	226.3 ± 0.3	221.5 ± 0.5	636.5 ± 4.5
Degraded	198.4 ± 0.3	186.2 ± 1.8	634.7 ± 1.8

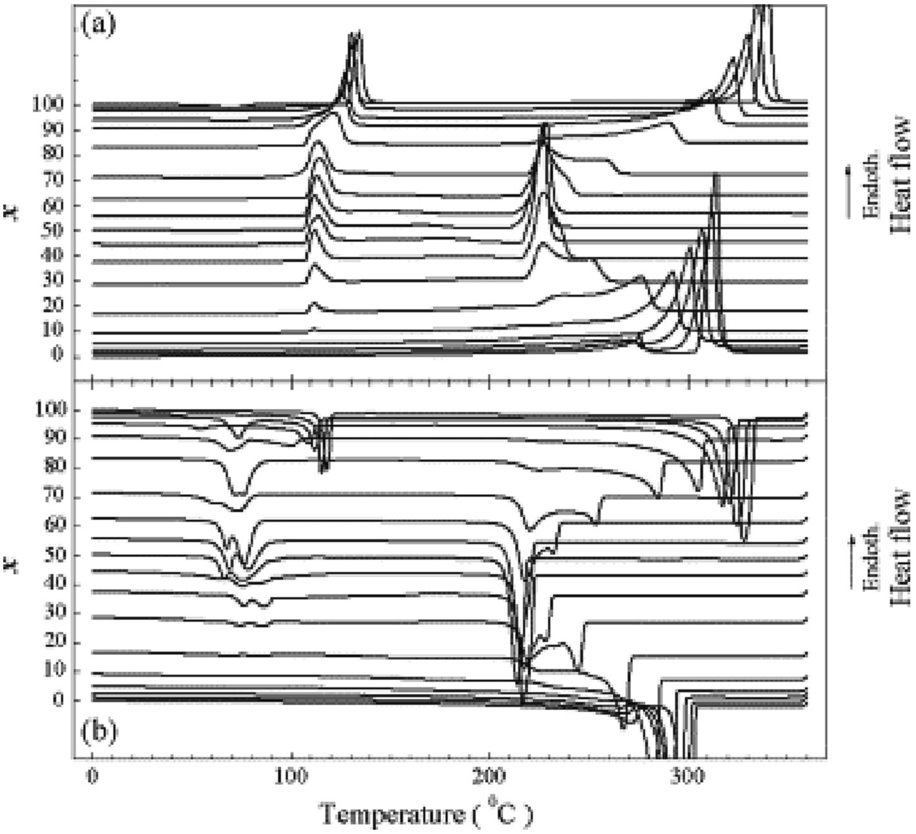

Fig. 9. DSC curves for the composition of $xKNO_3 + (100 - x)NaNO_3$ ($0 \leq x \leq 100$) measured during (a) heating at 20 °C/min and (b) cooling at 20 °C/min [10].

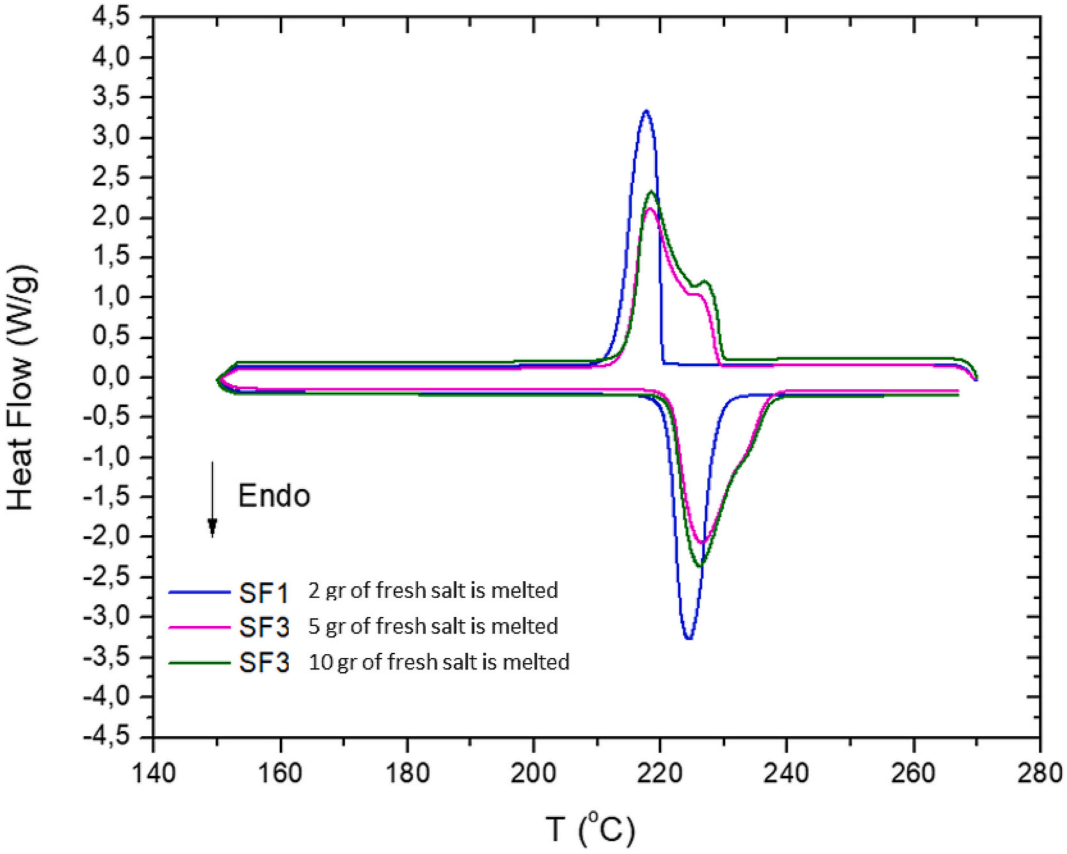

Fig. 10. DSC analysis of different quantities of untreated solar salt.

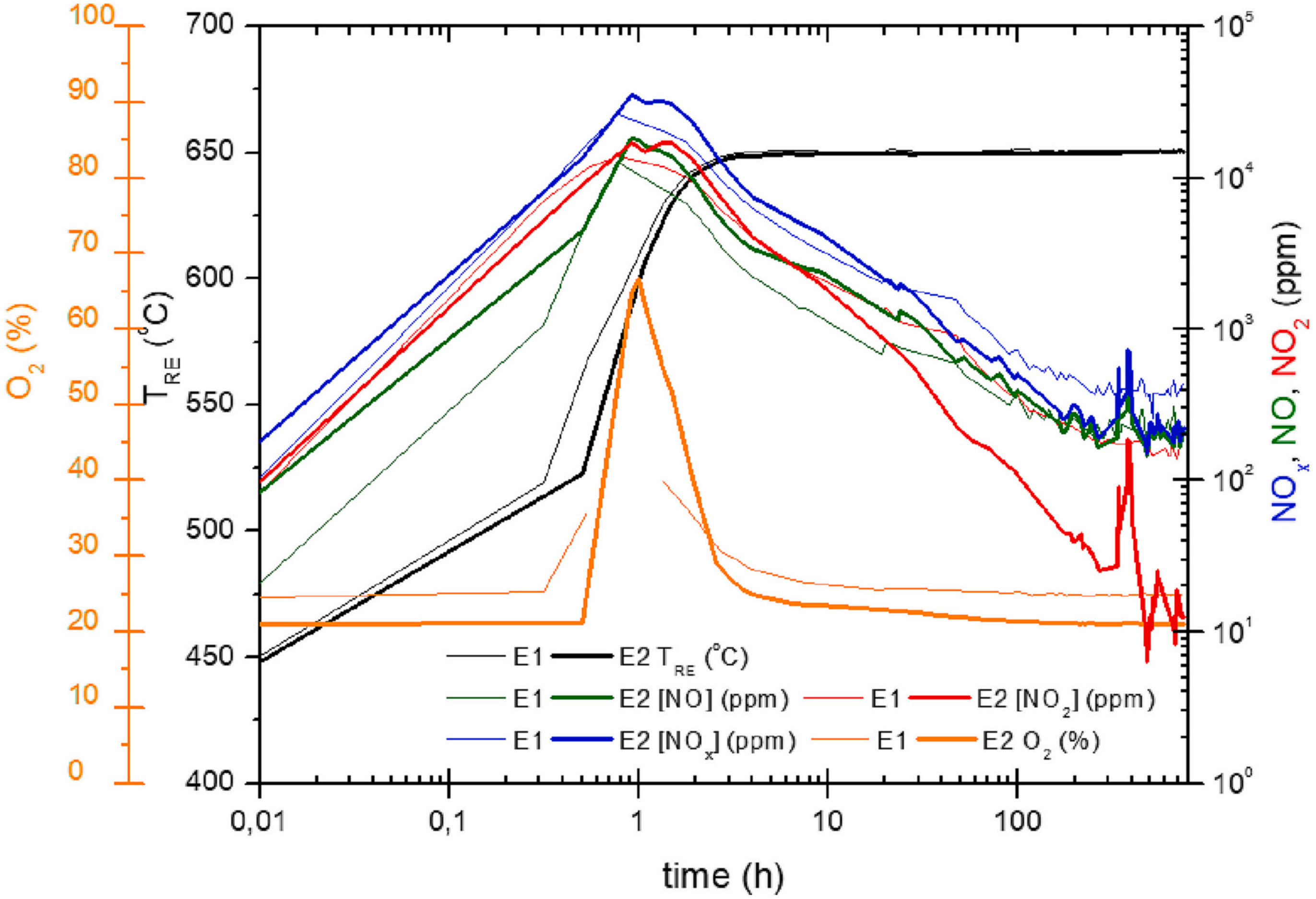

Fig. 11. Comparison of gases generated during treatment with oxygen as cover gas (E1) and dry air as cover gas (E2) during the heating treatment from 450 °C and 650 °C.

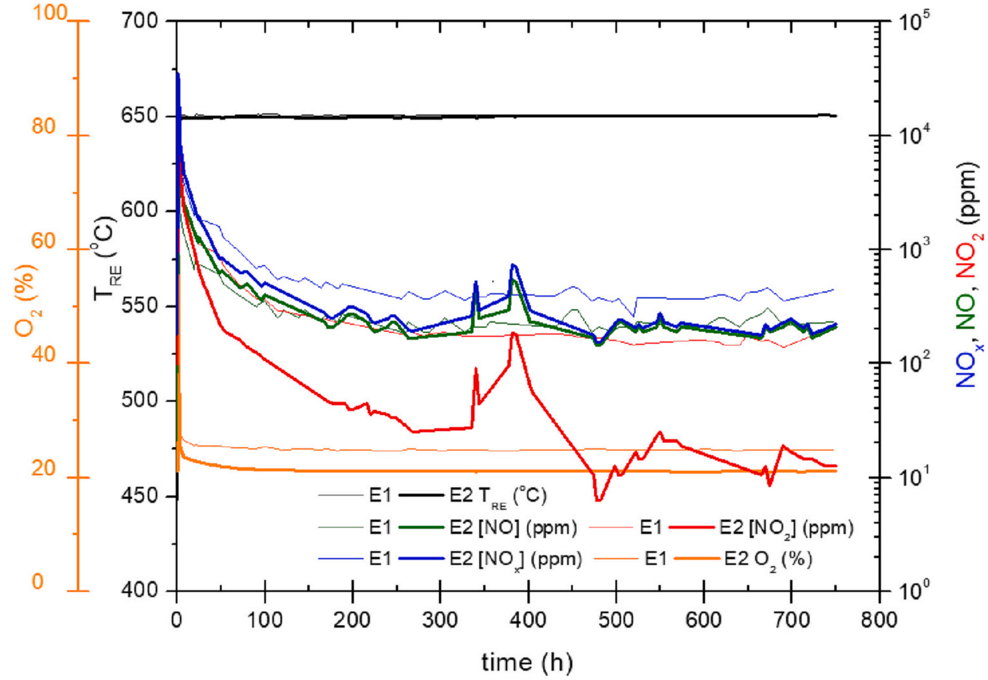

Fig. 12. Comparison of gases generated during treatment with oxygen as cover gas (E1) and dry air as cover gas (E2) during the heating treatment from at 650 °C.

Table 5
Nitrite content on degraded salt after treatment with oxygen as cover gas (E1) and dry air as cover gas (E2) at 650 °C.

Sample	Nitrites (ppm)
E1 – salt after treatment with oxygen as cover gas	35,422
E2 – salt after treatment with air as cover gas	99,508

The comparison of the TGA analysis in both experiments (Figs. 6a and 8a) does not give significant differences that could be attributed to salt degradation.

On the other hand, the comparison of DSC curves (Figs. 6b and 8b) shows a decrease in the melting temperature of the salt after treatment with both cover gases, but it is higher when dry air is used. This can be attributed to the emergence of nitrites and oxides that change the binary composition of the mixture [7].

5. Conclusions

A specific test was designed to analyse the effect of the cover gas in the degradation of the Solar Salt. To this end, two experiments were performed, one using dry air and another one oxygen, both at 650 °C. The obtained results showed that the use of oxygen as cover gas slow down the thermal decomposition of the solar salt, showing a reduction in the formation of NOx and nitrites. This fact was also validated by the smaller variation on the melting temperature of the degraded sample in an oxygen atmosphere.

The test performed confirm the viability of the use of oxygen as cover gas to increase the operation temperature of the molten salt without negatively impacting its composition on the long term.

CRediT authorship contribution statement

Cristina Prieto: Conceptualization, methodology, validation, funding acquisition, supervision and writing and reviewing.

Anton Lopez-Roman: Data curation and writing-reviewing.

Luisa F. Cabeza: Methodology, writing-reviewing and editing.

Declaration of competing interest

The authors declare that they have no known competing financial interests or personal relationships that could have appeared to influence the work reported in this paper.

Data availability

The data that has been used is confidential.

Acknowledgements

This work was partially funded by the Ministerio de Ciencia e Innovación de España [(ITC-20111061-FEDER-Innterconecta-Composol) (PID2021-123511OB-C31 - MCIU/AEI/FEDER, UE) (TED2021-132216A-I00)] and by the Ministerio de Ciencia, Innovación y Universidades - Agencia Estatal de Investigación (AEI) (RED2018-102431-T). The authors would like to thank the Department of Chemical Engineering in the University of Huelva. The authors at University of Lleida would like to thank the Catalan Government for the quality accreditation given to their research group GREiA (2017 SGR 1537). GREiA is a certified agent TECNIO in the category of technology developers from the Government of Catalonia. This work is partially supported by ICREA under the ICREA Academia programme.

References

[1] IRENA, Innovation Outlook: Thermal Energy Storage, 2020.
[2] M.T. Islam, N. Huda, A.B. Abdullah, R. Saidur, A comprehensive review of state-of-the-art concentrating solar power (CSP) technologies: current status and research trends, Renew. Sust. Energ. Rev. 91 (Ago. 2018) 987–1018, https://doi.org/10.1016/j.rser.2018.04.097.
[3] R.W. Bradshaw, S.H. Goods, Corrosion of Alloys and Metals by Molten Nitrates, Sandia National Lab. (SNL-CA), Livermore, CA (United States), Ago. 2001, https://doi.org/10.2172/1545803. SAND-2000-8727.
[4] K.H. Stern, High temperature properties and decomposition of inorganic salts part 3, nitrates and nitrites, J. Phys. Chem. Ref. Data 1 (3) (Jul. 1972) 747–772, https://doi.org/10.1063/1.3253104.
[5] D.A. Nissen, D.E. Meeker, Nitrate/nitrite chemistry in sodium nitrate-potassium nitrate melts, Inorg. Chem. 22 (5) (Mar. 1983) 716–721, https://doi.org/10.1021/ic00147a004.
[6] R.I. Olivares, The thermal stability of molten nitrite/nitrates salt for solar thermal energy storage in different atmospheres, Sol. Energy 86 (9) (2012) 2576–2583, https://doi.org/10.1016/j.solener.2012.05.025.
[7] C. Zhu, X. Cheng, Y. Li, B. Tao, Influence of heat treatment on solidus temperature of NaNO3–KNO3 molten salt, Sol. Energy 118 (Ago. 2015) 303–312, https://doi.org/10.1016/j.solener.2015.05.024.
[8] S. Wright, T. Tran, C. Chen, R. Olivares, S. Shouyi, Thermal stability of potassium and sodium nitrate molten salt mixtures above 500 °C, in: 9th International Conference on Molten Slags, Fluxes and Salts (MOLTEN12), Chinese Society for Metals, Beijing, China, 2012 (p. Paper W074 (14p)).
[9] C. Prieto, et al., Effect of the impurity magnesium nitrate in the thermal decomposition of the solar salt, Sol. Energy 192 (Nov. 2019) 186–192, https://doi.org/10.1016/j.solener.2018.08.046.
[10] W. Ping, P. Harrowell, N. Byrne, C.A. Angell, Composition dependence of the solid state transitions in NaNO3/KNO3 mixtures, Thermochim. Acta 486 (1–2) (Mar. 2009) 27–31, https://doi.org/10.1016/j.tca.2008.12.017.